



This is a repository copy of *Characterization of multi-layered tissue engineered human alveolar bone and gingival mucosa*.

White Rose Research Online URL for this paper:

<https://eprints.whiterose.ac.uk/123618/>

Version: Accepted Version

Article:

Almela, T., Al-Sahaf, S., Bolt, R. et al. (2 more authors) (2018) Characterization of multi-layered tissue engineered human alveolar bone and gingival mucosa. *Tissue Engineering Part C: Methods*, 24 (2). pp. 99-107. ISSN 1937-3384

<https://doi.org/10.1089/ten.TEC.2017.0370>

Final publication is available from Mary Ann Liebert, Inc., publishers
<http://dx.doi.org/10.1089/ten.TEC.2017.0370>

Reuse

Items deposited in White Rose Research Online are protected by copyright, with all rights reserved unless indicated otherwise. They may be downloaded and/or printed for private study, or other acts as permitted by national copyright laws. The publisher or other rights holders may allow further reproduction and re-use of the full text version. This is indicated by the licence information on the White Rose Research Online record for the item.

Takedown

If you consider content in White Rose Research Online to be in breach of UK law, please notify us by emailing eprints@whiterose.ac.uk including the URL of the record and the reason for the withdrawal request.



eprints@whiterose.ac.uk
<https://eprints.whiterose.ac.uk/>



This is an author produced version of *Characterization of Multi-layered Tissue Engineered Human Alveolar Bone and Gingival Mucosa*.

White Rose Research Online URL for this paper:
<http://eprints.whiterose.ac.uk/123618/>

Article:

almela, T, Al-Sahaf, S, bolt, R et al. (2 more authors) (2017) Characterization of Multi-layered Tissue Engineered Human Alveolar Bone and Gingival Mucosa. *Tissue Engineering, Part C, Methods*. ISSN 1937-3384 (In Press)

<https://doi.org/10.1089/ten.TEC.2017.0370>

Tissue Engineering

Tissue Engineering Manuscript Central: <http://mc.manuscriptcentral.com/ten>

Characterization of Multi-layered Tissue Engineered Human Alveolar Bone and Gingival Mucosa

Journal:	<i>Tissue Engineering</i>
Manuscript ID	Draft
Manuscript Type:	Methods Article - Part C
Date Submitted by the Author:	n/a
Complete List of Authors:	Almela, Thafar; University of Sheffield Faculty of Medicine Dentistry and Health, The School of Clinical Dentistry, Academic Unit of Oral & Maxillofacial Medicine & Surgery Alsahaf, Sarmad; University of Sheffield Faculty of Medicine Dentistry and Health, The School of Clinical Dentistry, Academic Unit of Oral & Maxillofacial Medicine & Surgery Bolt, Robert; University of Sheffield Faculty of Medicine Dentistry and Health, The School of Clinical Dentistry, Academic Unit of Oral & Maxillofacial Medicine & Surgery Brook, Ian; University of Sheffield Faculty of Medicine Dentistry and Health, The School of Clinical Dentistry, Academic Unit of Oral & Maxillofacial Medicine & Surgery Moharamzadeh, K. ; University of Sheffield Faculty of Medicine Dentistry and Health, The School of Clinical Dentistry, Academic Unit of Restorative Dentistry
Keyword:	Bone < Applications in Tissue Engineering (DO NOT select this phrase; it is a header ONLY), 3-D Cell Culture < Enabling Technologies in Tissue Engineering (DO NOT select this phrase; it is a header ONLY), Composite Tissues < Applications in Tissue Engineering (DO NOT select this phrase; it is a header ONLY)
Manuscript Keywords (Search Terms):	Bone engineering, oral mucosa engineering, alveolar bone mucosal model, composite tissue engineering
Abstract:	Advances in tissue engineering have permitted assembly of multi-layered composite tissue constructs for potential applications in the treatment of combined hard and soft tissue defects and as an alternative in vitro test model to animal experimental systems. The aim of this study was to develop and characterize a novel three-dimensional combined human alveolar bone and gingival mucosal model based on primary cells isolated from the oral tissues. Bone component of the model was engineered by seeding primary human alveolar osteoblasts (HAOBs) into a hydroxyapatite/tricalcium phosphate (HA/TCP) scaffold and culturing in a spinner bioreactor. The engineered bone was then laminated, using an adhesive tissue sealant, with tissue engineered gingival mucosa consisting of air/liquid interface-cultured normal human gingival keratinocytes on oral fibroblast-populated collagen gel scaffold. Histological characterization revealed a structure consisting of established epithelial, connective tissue,

1
2
3
4
5
6
7
8
9
10
11
12
13
14
15
16
17
18
19
20
21
22
23
24
25
26
27
28
29
30
31
32
33
34
35
36
37
38
39
40
41
42
43
44
45
46
47
48
49
50
51
52
53
54
55
56
57
58
59
60

	<p>and bone layers closely comparable to normal oral tissue architecture. The mucosal component demonstrated a mature epithelium undergoing terminal differentiation similar to that characteristic of native buccal mucosa, as confirmed using cytokeratin 13 (CK13) and cytokeratin 14 (CK14) immunohistochemistry. Ultrastructural analysis confirmed the presence of desmosomes and hemi-desmosomes in the epithelial layer, a continuous basement membrane and newly synthesized collagen in the connective tissue layer. Quantitative PCR (qPCR) assessment of osteogenesis-related gene expression showed a higher expression of genes encoded Collagen I (COL1) and Osteonectin (ON) as well as Osteocalcin (OC), Osteopontin (OPN), and Alkaline phosphatase (ALP). ELISA quantification of collagen I, ON, and OC confirmed a pattern of secretion which paralleled the model's gene expression profile. We demonstrate here that replicating the anatomical setting between oral mucosa and the underlying alveolar bone is feasible and the developed model showed characteristics similar to those of normal tissue counterparts. This tri-layered model therefore offers great scope as an advanced, and anatomically-representative tissue-engineered alternative to animal models.</p>

SCHOLARONE™
Manuscripts

Not for Distribution

1
2
3 **Characterization of Multi-layered Tissue Engineered Human Alveolar Bone and**
4
5 **Gingival Mucosa**
6
7

8 Thafar Almela*, Sarmad Al-Sahaf, Robert Bolt, Ian M. Brook, Keyvan Moharamzadeh *

9
10 School of Clinical Dentistry, University of Sheffield, Claremont Crescent, Sheffield, S10
11
12 2TA UK
13

14
15
16 **Corresponding authors:*
17

18
19 Tkalmela1@sheffield.ac.uk
20

21
22 K.moharamzadeh@Sheffield.ac.uk
23

24
25
26 Thafar Almela; BDS, MSc
27

28
29 University of Sheffield, School of Clinical Dentistry, 19 Claremont Crescent, Sheffield
30
31 S10 2TA
32

33
34 Telephone: +44 (0) 7476828728
35

36
37 Email: Tkalmela1@sheffield.ac.uk
38
39

40
41 Sarmad Al-Sahaf; BDS, MSc
42

43
44 University of Sheffield, School of Clinical Dentistry ,19 Claremont Crescent, Sheffield, S10
45
46 2TA
47

48
49 Telephone: +44 (0)7425059153
50

51
52 Email: sshal-sahaf1@sheffield.ac.uk
53

54 Robert Bolt; BDS (Hons), MFDS, MBChB (Hons), MCLinRes PhD, MOraISurg.
55

56
57 University of Sheffield, School of Clinical Dentistry 19 Claremont Crescent, Sheffield,
58
59 S10 2TA
60

1
2
3 Telephone: +44(0)114 2265463
4

5 Email: r.bolt@sheffield.ac.uk
6
7
8

9 Ian M. Brook; BDS MDS FDSRCS(Eng) PhD
10

11 The School of Clinical Dentistry, University of Sheffield, 19 Claremont Crescent, Sheffield
12 S10 2TA
13

14
15 Telephone: +44(0) 1142717851
16

17 Email: i.brook@sheffield.ac.uk
18
19
20

21 Keyvan Moharamzadeh; BSc, DDS, PhD, FHEA, FDSRCS
22

23 The School of Clinical Dentistry, University of Sheffield, 19 Claremont Crescent, Sheffield
24 S10 2TA
25
26

27
28 Telephone: +44(0) 1142717910
29

30 Email: K.moharamzadeh@sheffield.ac.uk
31
32
33
34

35 The study was performed in School of Clinical Dentistry, University of Sheffield, Claremont
36 Crescent, Sheffield, S10 2TA UK.
37
38
39
40
41
42
43
44
45
46
47
48
49
50
51
52
53
54
55
56
57
58
59
60

Abstract

Advances in tissue engineering have permitted assembly of multi-layered composite tissue constructs for potential applications in the treatment of combined hard and soft tissue defects and as an alternative in vitro test model to animal experimental systems. The aim of this study was to develop and characterize a novel three-dimensional combined human alveolar bone and gingival mucosal model based on primary cells isolated from the oral tissues. Bone component of the model was engineered by seeding primary human alveolar osteoblasts (HAOBs) into a hydroxyapatite/tricalcium phosphate (HA/TCP) scaffold and culturing in a spinner bioreactor. The engineered bone was then laminated, using an adhesive tissue sealant, with tissue engineered gingival mucosa consisting of air/liquid interface-cultured normal human gingival keratinocytes on oral fibroblast-populated collagen gel scaffold. Histological characterization revealed a structure consisting of established epithelial, connective tissue, and bone layers closely comparable to normal oral tissue architecture. The mucosal component demonstrated a mature epithelium undergoing terminal differentiation similar to that characteristic of native buccal mucosa, as confirmed using cytokeratin 13 (CK13) and cytokeratin 14 (CK14) immunohistochemistry. Ultrastructural analysis confirmed the presence of desmosomes and hemi-desmosomes in the epithelial layer, a continuous basement membrane and newly synthesized collagen in the connective tissue layer. Quantitative PCR (qPCR) assessment of osteogenesis-related gene expression showed a higher expression of genes encoded Collagen I (COL1) and Osteonectin (ON) as well as Osteocalcin (OC), Osteopontin (OPN), and Alkaline phosphatase (ALP). ELISA quantification of collagen I, ON, and OC confirmed a pattern of secretion which paralleled the model's gene expression profile. We demonstrate here that replicating the anatomical setting between oral mucosa and the underlying alveolar bone is feasible and the developed model showed characteristics similar to those of normal tissue counterparts. This tri-layered model therefore offers great scope as an advanced, and anatomically-representative tissue-engineered alternative to animal models.

Keywords: Bone engineering, oral mucosa engineering, alveolar bone mucosal model, composite tissue engineering.

1. Introduction

The orofacial region is a highly complex anatomical structure, comprising a large number of tissue types within a relatively small area. Restoration of defects following trauma, excision of pathology, and in the correction of developmental deformities, poses a great challenge due to the lack of suitable donor sites for harvesting grafts capable of accurately replicating the missing tissues. Whilst the need for anatomically-accurate grafting materials offers a niche that could be filled using refined tissue engineered constructs, it also imposes a considerable challenge to current composite tissue engineering techniques in order to create and attach the numerous tissue types required to replicate the normal anatomy of this region.⁽¹⁾ Despite this challenge, 3D *in vitro* screening systems, based on human cells and tissues, have already attracted significant attention, as they offer more robust and predictive experimental data compared to 2D or animal models.⁽²⁾ Limitations of 2D models include the loss of a natural 3D environment, which is in turn reflected in cell behaviour,⁽³⁾ and additionally the absence of a 3D environment excludes important factors such as hypoxic gradients and drug penetration. Furthermore, animal studies may be misleading due to interspecies molecular and physiological differences.⁽⁴⁾ Therefore, the short-term need for anatomically-representative 3D models of the oro-facial region is assured. Future development of these models beyond experimental analysis furthermore offers potential to achieve the longer-term goal of establishing tissue engineered grafting materials capable of improving and simplifying the reconstruction of surgical defects in the orofacial region.

Over the last few decades, there has been a substantial amount of innovation and progress in the engineering of various tissues found in the orofacial region, such as cartilage, bone, mucosa, and periodontium.⁽⁵⁾ This has encouraged researchers to develop more intricately-structured hybrid tissues that differ in the characteristics of their constituent parts, yet comprise a single functional unit. To date, only a few examples of composite tissues have

1
2
3 been engineered which replicate the orofacial region. Recent successes include the
4
5 engineering of osteochondral components of the temporomandibular joint, which comprises
6
7 both articular cartilage and subchondral bone; ^(6, 7) and the engineering of a ligamentous
8
9 interface between tooth and alveolar bone to replicate the bone-periodontal ligament
10
11 complex. ⁽⁸⁾

12
13
14 Despite these advances, the three key components of the majority of orofacial tissues are that
15
16 of bone, fibrous connective tissue and an overlying epithelium. Development of an accurate
17
18 alveolar bone-mucosal model therefore represents another important step in the process of
19
20 achieving a clinically utilisable tissue engineered orofacial construct. We previously reported
21
22 the feasibility of tissue engineering such a model using cancer and immortal cell lines, ⁽⁹⁾
23
24 although acknowledged that patient-sourced primary cells are essential for such a model to be
25
26 developed to create a more accurate representation of native tissue.
27
28
29

30
31 The aim of this study was to develop a novel three-dimensional combined human alveolar
32
33 bone and gingival mucosal model based on primary cells isolated from the native human oral
34
35 hard and soft tissues and to characterize this model qualitatively and quantitatively to
36
37 examine whether it accurately replicates the normal tissues in terms of histology,
38
39 ultrastructural appearance, differentiation and phenotype characteristics.
40
41
42
43
44
45
46
47
48
49
50
51
52
53
54
55
56
57
58
59
60

2. Materials and Methods

2.1. Study design

Gingival biopsies and bone chips were obtained with written, informed consent from patients undergoing elective oral surgery at Charles Clifford Dental Hospital, Sheffield, UK, under appropriate ethical approval from National Research Ethics Services Committee (number 15/LO/0116). The study included simultaneous tissue engineering of oral mucosal model (OMM) and bone model (BM), then combining both to form a composite alveolar bone mucosal model (ABMM) (Figure1). All materials were purchased from Sigma Aldrich, UK unless otherwise stated.

2.2. Isolation and cultivation of primary human gingival cells

Normal human oral keratinocytes (NHOKs) and normal human oral fibroblasts (NHOFs) were isolated from gingival biopsies as previously described with some modifications.⁽¹⁰⁾ Briefly, the gingival tissues were collected and kept for 4-5 hours at 4°C in transport medium consisting of serum free Dulbecco's Modified Eagles Medium (DMEM)-GlutaMAX™ (Gibco, USA) supplemented with 100 IU:100 mg ml⁻¹ penicillin-streptomycin (P/S) and 625 ng ml⁻¹ fungizone. NHOKs were then enzymatically isolated from the biopsies by incubating the tissue in 0.25% trypsin-EDTA for 14-16 hours at 4°C. The epithelial layer was then scraped, cut into small pieces, and plated in 25 cm² tissue culture flask at a density of 1.5×10⁶ with an equal number of i3T3 feeder layer fibroblasts. The keratinocytes were then cultured in a humidified atmosphere of 5 % CO₂ /95 % air at 37 °C in Green's medium.⁽¹¹⁾

NHOFs were isolated from the connective tissue layer by incubating in 0.05% (w/v) collagenase type I (Gibco, USA) in DMEM-GlutaMAX™ containing 10% Fetal bovine serum (FBS) at 37 °C for 4 hours. The digested tissue was then centrifuged at 200 g for 5 minutes, and the resultant pellet re-suspended in complete DMEM (CDMEM; DMEM-

1
2
3 GlutaMAX™ supplemented with 10% FBS, 625 ng/mL fungizone, and 100 IU:100 mg ml⁻¹
4
5 P/S).
6
7

8 Both NHOKs and NHOFs were fed three times a week until confluency and then used at
9
10 passage 2.
11

12 13 **2.3. Isolation and cultivation of primary human alveolar osteoblasts**

14
15
16 Primary human alveolar osteoblasts (HAOBs) were isolated from bone chips collected in a
17
18 sterile bone trap during preparation of dental implant sites.^(12, 13) After collection in transport
19
20 medium, the osseous tissues were extensively rinsed in phosphate buffered saline (PBS) and
21
22 vortexed to remove blood components. Bone fragments were cultured as explants in 75 cm²
23
24 flask in CDMEM supplemented with 50 µg/ml L-ascorbic acid 2-phosphate (L-AA) at 37°C
25
26 in a humidified atmosphere of 95% air, 5% CO₂. The culture was left undisturbed for 7 days,
27
28 after which the medium was replaced 2-3 times/week until the culture attained confluency,
29
30 whereby cells were detached by trypsin/EDTA (0.25%), sub cultured, and used in the 3nd
31
32 passage.
33
34
35

36 37 **2.4. Engineering the oral mucosal models (OMMs)**

38
39
40 Collagen-based OMM was constructed according to the technique described by Dongari-
41
42 Bagtzoglou and Kashleva.⁽¹⁴⁾ A solution of 10 × DMEM 13.8 mg ml⁻¹, FBS 8.5% (v/v), L-
43
44 glutamine 2 mM, reconstitution buffer (22 mg ml⁻¹ sodium bicarbonate and 20 mM HEPES),
45
46 and 5 mg ml⁻¹ rat-tail type I collagen (R & D system) was prepared on ice and neutralized by
47
48 1M sodium hydroxide to pH=7.4.
49

50
51 Finally, a cell suspension of NHOFs in CDMEM at a concentration of 2×10⁵ cells per model
52
53 was added to the solution. The resultant fibroblast-containing collagen was transferred into
54
55 tissue culture inserts (0.4 µm pore size, 30 mm diameter, Millipore) and incubated at 37°C
56
57 for 2 hours until solidified. 1.5 ml CDMEM was then added inside and outside the insert.
58
59
60

1
2
3 After 3 days, 1×10^6 NHOK cells (per model) suspended in 50 μ l Green's medium were
4 seeded on the gel surface and allowed to adhere for 3 hours. 2 ml Green's medium was then
5
6 gently added into the insert and incubated at 37 °C, 5% CO₂ for 4 days. When epithelial cells
7
8 reached confluency, the culture was raised to air/liquid interface and fed every other day for
9
10 10 days.
11
12

13 14 15 **2.5. Engineering the bone models (BMs)**

16
17 10 sterile ceramic discs (2mm \times 10mm) of Hydroxyapatite/Tricalcium phosphate (HA/TCP)
18 (60%/40%) (Ceramisys LTD, UK) with total porosity of 78.9 % were used as a scaffold. The
19 discs were placed in 24- well plates and pre-wetted with CDMEM 24 hours before cell
20 seeding. 2×10^6 HOBs cells suspended in 15 μ l CDMEM /L-AA were then added dropwise to
21 each scaffold. The cells were allowed to adhere for 2 hours, and then BMs completely
22 covered with 2 ml CDMEM /L-AA and incubated overnight. After 24 hours, BMs were
23 suspended in a spinner bioreactor (Branstead Stem, UK) and spun at a rate of 30 rpm. The
24 medium was changed every 2 days for 17 days.
25
26
27
28
29
30
31
32
33
34
35

36 **2.6. Cell viability assessment using PrestoBlue (PB) live assay**

37
38
39 The assessment of cell viability within BMs and OMMs was performed using the PB assay
40 (Invitrogen, USA) at day 17 before the combination of the two constructs. BMs and OMMs
41 were separately placed in a 12- well tissue culture plate, washed with PBS, and then a
42 mixture of 900 μ l of CDMEM and 100 μ l of PB reagent was added to each well. Three
43 acellular discs and collagen gel were included as negative controls for BMs and OMMs,
44 respectively. After 3 hours incubation at 37°C, the fluorescence values (excitation/emission:
45 560/590 nm) of 200 μ l aliquot were measured in triplicates using spectrophotometric plate
46 reader (Infinite® M200, TECAN, USA). For calculation, the average fluorescence values of
47
48
49
50
51
52
53
54
55
56
57
58
59
60

1
2
3 the medium containing the scaffolds without cells were subtracted from the averaged sample
4
5 readings.
6
7
8
9
10
11
12
13

14 **2.7. Engineering the composite alveolar bone mucosal models (ABMMs)**

15
16 ABMMs were constructed as previously described.⁽⁹⁾ At day 17, BM and OMM models were
17
18 combined using a biocompatible fibrin-based adhesive sealant (ARTISS, Baxter, UK). In
19
20 brief, BMs were retrieved and placed on a sterile culture plate containing 10 ml CDMEM.
21
22 The fibrin adhesive was prepared in a pre-filled syringe according to manufacturer's
23
24 instructions, and a thin layer of the mixed fibrinogen-thrombin sealer applied to the non-
25
26 epithelial side of an OMM. The OMM was then immediately attached to the surface of a BM
27
28 and held in the desired position with gentle compression for a minimum of 60 seconds to
29
30 ensure the adhesive material had completely set, and that both models were firmly adhered to
31
32 each other. The ABMMs were then further cultured for 5 days, after which the analyses were
33
34 performed.
35
36
37
38

39 **2.8. Histological examination of ABMM**

40
41 ABMMs were fixed in 4% paraformaldehyde (PFA) for 24 hours and embedded in 2-
42
43 hydroxyethyl methacrylate resin (Technovit 7100, Heraeus Kulzer) according to
44
45 manufacturer's instructions. Briefly, samples were dehydrated in graded ethanol series 75%,
46
47 95%, 100% for at least 2 hours, then pre-infiltrated with equal parts of basic solution and
48
49 100% ethanol overnight on a rotating mixer. Infiltration was performed with infiltration
50
51 medium consisting of 100 ml basic solution and 1 g Hardener1. Finally, samples were
52
53 polymerized in suitable molds with premixed 15 ml infiltration medium and 1 ml Hardener-
54
55 2. Polymerisation was completed over the period of 2 hours at room temperature.
56
57
58
59
60

1
2
3 For routine haematoxylin and eosin (H&E) staining (Leica Microsystems), the ground block
4 was first sectioned into 100-150 μm thickness with a cutting machine (IsoMet[®] 1000
5 precision saw, Buehler UK Ltd, UK). The section was then adhered to a glass slide using
6 cyanoacrylate adhesive (Loctite[®] glass bond UV curing, UK). The thickness was then further
7 reduced to 30-35 μm by grinding the sections with silicon carbide papers of P800 and P1200
8 roughness in a grinder-polisher machine (Buehler[™] Metaserv, UK).
9
10
11
12
13
14
15

16 17 **2.9. Histological, Immunofluorescent (IF), and Transmission Electron Microscopy** 18 **(TEM) Examinations of OMMs.** 19

20
21
22 OMMs were processed for histological, IF, and TEM examination at the end of culture
23 period. Frozen sections were prepared as previously described.⁽¹⁵⁾ OMM were fixed with 4%
24 PFA for 24 hours, followed by an overnight incubation in 18% sucrose in PBS. The samples
25 were frozen in OCT Compound (Thermofisher) and sectioned to 14 μm , and sections were
26 then either stained with H&E for examination under inverted microscope (Olympus, Japan),
27 or were subjected to IF staining.
28
29
30
31
32
33
34
35

36 For IF staining, the sections were washed with PBS for 5 minutes, permeabilized with 0.2 %
37 Triton x-100 for 5 minutes, and then blocked with 1% bovine serum albumin (BSA) in 0.1 %
38 PBS-Tween for 1 hour. The sections were then incubated overnight at 4 °C with conjugated
39 anti-Cytokeratin 13 (Abcam, UK, ab198584) and anti-Cytokeratin 14 (Abcam, UK,
40 ab192055) antibodies at a working dilution of 1:100. After washing, slides were mounted
41 using DAPI-containing mounting medium (Thermofisher, UK) and viewed using IF
42 microscopy (Zeiss Ltd, Germany). Normal oral mucosa (NOM) was used as a positive
43 control, while negative control was OMM stained with IgG isotype (1:100) (ebioscience,
44 UK), followed by goat anti rabbit secondary antibodies (1:200) (Abcam, UK, ab150083).
45
46
47
48
49
50
51
52
53
54
55
56
57
58
59
60

1
2
3 For TEM analysis, 4mm sections of OMM were fixed in 3% glutaraldehyde in 0.1 M sodium
4 cacodylate buffer for 2 hours at 4°C, and post fixed in 1% osmium tetroxide for 2 hours.

5
6 Tissue was dehydrated with 70%, 95%, and 100% ethanol and then embedded in resin.
7
8 Samples were left for 48 hours in the oven at 60 °C, and thereafter examined using a
9
10 transmission electron microscope (FEI tecnai 12 Bio-twin, 120Kv TEM).
11
12

13 14 **2.10. Quantitative polymerase chain reaction (qPCR) examination**

15
16 For gene expression analysis, ABMMs were snap frozen, grinded, and digested with lysis
17 buffer. RNA was isolated using isolate II RNA Mini Kit (BioLine, UK) according to
18 manufacturer's instructions. 500 ng total RNA was reverse transcribed using a High-Capacity
19 RNA to Complementary DNA (cDNA) kit (Life Technologies, UK).
20
21

22
23 0.5 µl cDNA was amplified using 5 µl TaqMan gene expression master mix, 3.5 µl nuclease
24 free water and 0.5 µl TaqMan gene probes (Applied Biosystems). Genes encoding the
25 following markers were then interrogated; ALP, Osteopontin (OP), Osteonectin (ON),
26
27 Osteocalcin (OC), Collagen I (COL1), Ki 67, Cytokeratin 10 (CK10), and Cytokeratin 13
28 (CK13). B-2-Microglobulin was used as a reference control gene (All Applied biosystem,
29
30 UK).
31
32

33
34 Cycling conditions were holding at 95°C for 10 minutes, then 95°C for 10 seconds, followed
35 by 60 °C for 45 seconds and the cycle was repeated 40 times (QIAGEN, Germany). The
36
37 threshold cycle (Ct) was normalized against the reference gene (Δ Ct) and the expression
38
39 relative to it was calculated.
40
41
42
43
44
45
46
47

48 49 **2.11. Enzyme-linked immunosorbent assay (ELISA)**

50
51 Commercially available ELISA kits for COL1, ON (R&D systems, UK), and OC (Abcam,
52
53 UK) were used according to manufacturer's instructions in order to quantify these proteins in
54
55 ABMM after 24 hours incubation in serum free tissue culture conditioned medium. The
56
57
58
59
60

1
2
3 solutions were read at absorbance 450 nm using a microplate reader (Infinite® M200,
4
5 TECAN, USA).

6 7 **2.12. Statistics**

8
9 All data were presented in terms of mean \pm SD of three independent experiments performed
10
11 in triplicate. One-way ANOVA complemented by Tukey's multiple comparisons test was
12
13 performed using GraphPad Prism v7.0 (GraphPad Software, La Jolla, CA), and differences
14
15 were considered significant when $p < 0.05$.

16 17 **3. Results**

18 19 **3.1. Viability assay**

20
21 Cell viability testing using the PB assay revealed that HAOBs within the bone model as well
22
23 as NHOFs and NHOKs in the OMM remained vital throughout the experiment (Figure 2).
24
25

26 27 **3.2. Histological assessment of ABMM**

28
29 Histological observation revealed that the ABMM had a structure consisting of epithelial,
30
31 connective tissue and bony layers which were comparable to the histological architecture of
32
33 the soft and hard tissues of the oral cavity (Figure 3A). The model's surface displayed a
34
35 continuous stratified epithelial layer, and a connective tissue layer densely populated with
36
37 viable fibroblasts (Figure 3B). The hard-soft tissue interface showed a thin band of cell-
38
39 infiltrated sealant adhering both layers (Figure 3C). Viable cells evenly populated the
40
41 scaffold porosities with a secreted matrix partially or completely filling the pores of the
42
43 scaffold (Figure 3D).
44
45

46 47 **3.3. OMM assessments**

48
49 Histologically, the OMM showed a proliferating basal layer and well-differentiated stratified
50
51 squamous oral epithelium of 12-14 NHOKs thickness, which mimicked that of NOM (Figure
52
53 4). The epithelium consisted of four distinct layers that included equivalents to basal, spinous,
54
55 intermediate, and superficial cells, respectively. The uppermost aspect of the superficial layer
56
57
58
59
60

1
2
3 had cells of a flattened appearance, while cells in the basal layer remained rounded. Glycogen
4
5 granules were occasionally observed in the intermediate layer. NHOFs were found dispersed
6
7 homogeneously in the connective tissue.
8

9
10 Figure 5 shows the keratin expression of NOM and OMM, as assessed by immunofluorescent
11
12 staining for CK13 and CK14. The suprabasal cells of the OMM strongly expressed CK13,
13
14 consistent with the staining of intermediate and superficial cells in para-keratinized stratified
15
16 epithelium.⁽¹⁶⁾ CK14 was expressed throughout the entire epithelium.
17

18
19 Ultrastructural analysis of the OMM demonstrated the presence of numerous desmosomes
20
21 between adjacent epithelial cells (Figure 6A). A continuous and intact basement membrane
22
23 was formed, anchoring the epithelium firmly to the connective tissue by means of
24
25 hemidesmosomal attachments (Figure 6B). In the sup-epithelial layer, a high amount of
26
27 newly synthesized collagen was observed (Figure 6C).
28

29 30 **3.4. qPCR assessment**

31
32 Figure (7) summarises gene expression for the composite model, including both HAOB and
33
34 NHOK cell components. Of all genes evaluated, COL1 demonstrated the highest level of
35
36 expression. Bone-specific genes such as ALP, OC, ON, and OP were detected, with ON
37
38 expressed in high quantities. Genes encoding CK10 and CK13 were expressed, and were not
39
40 significantly different.
41
42

43 44 **3.5. ELISA**

45
46 ELISA results for COL1, ON, and OC were consistent with the qPCR findings. COL1
47
48 demonstrated a significantly increased protein concentration in comparison to ON and OC.
49
50 ON, in turn, was higher than OC (Figure 8).
51
52

53 54 **4. Discussion**

1
2
3 There is an increasingly recognized need to engineer tissue equivalents for both clinical
4
5 and experimental applications. In this study, we have developed and characterized an *in vitro*
6
7 3D human alveolar osteomucosal construct that replicates the natural anatomical relationship
8
9 of oral mucosal tissue and the underlying bone.
10

11
12 In 3D culture, cell viability is influenced by several factors including the scaffold and culture
13
14 environment. Calcium phosphate and collagen constitute the main elements of the
15
16 extracellular matrix of bone and oral mucosa, respectively.⁽¹⁷⁾ Therefore, due to their
17
18 biocompatibility, they have been widely used in tissue engineering as scaffolds to support
19
20 cells growth without compromising their vitality.⁽¹⁸⁾ The culture environment, on the other
21
22 hand, that promotes mass transfer and nutrient delivery is another important factor to
23
24 maintain cell vitality. In our study, growing OMM in a static culture raised no problem due to
25
26 the hydrophilic, high water-containing networks of collagen hydrogel that enhance
27
28 permeability for oxygen, nutrients and water-soluble metabolites.⁽¹⁹⁾ Ceramic-based bone
29
30 model, by contrast, required a dynamic flow to improve nutrient and waste diffusion because
31
32 the static culture is only sufficient to nourish the thin superficial layer, approximately 100-
33
34 200 μ m, contacting the medium.⁽²⁰⁾ As the cells increase in number, so does their metabolic
35
36 demand and the build-up of waste products. Consequently, the deeper cells in the tissue
37
38 interior can be deprived of oxygen and nutrients source in long-term static culture conditions.
39
40 For this reason, the total culture time of the composite tissue after combining the hard and
41
42 soft tissue constructs was limited to an additional 5 days at the static air/liquid interface in
43
44 this study.
45
46
47
48
49
50

51 We have shown that the histological structure and expression of key markers of epithelial
52
53 differentiation in OMM were comparable to those of its normal tissue counterpart. OMM
54
55 displayed the characteristics of a para-keratinized epithelium, which suggests that the
56
57
58
59
60

1
2
3 keratinocytes used in this model retain the para-keratinized status of the original oral mucosa
4
5 from which they were derived.⁽²¹⁾
6
7

8 The control of keratinocyte in proliferation and differentiation is multifactorial. Several
9
10 studies have confirmed the role of fibroblasts in epithelial development through the
11
12 stimulation of keratinocyte proliferation, migration, and keratin expression.^(22, 23) Fibroblasts
13
14 establish such growth-promoting roles through paracrine cross talk between NHOFs and
15
16 NHOKs via cytokines such as heparin-binding EGF-like growth factor (HB-EGF),
17
18 Interleukin 1 alpha (IL-1 α) and Transforming growth factor beta 1 (TGF- β 1).⁽²⁴⁾ This
19
20 function requires an optimal fibroblast density, as the presence of either excessive or
21
22 inadequate numbers of fibroblast will adversely affect epithelium morphogenesis, leading to
23
24 differentiation markers being inappropriately expressed.⁽²⁵⁾ In our models, optimal fibroblast
25
26 seeding density in order to support an anatomically representative epithelial layer was found
27
28 to be 2×10^5 cells per model. Keratinocyte senescence may also impact on the capacity to
29
30 achieve anatomically representative epithelia in tissue culture models. Due to sustained
31
32 telomerase expression within primary cells, sequential sub culturing may restrict the capacity
33
34 of keratinocytes to divide once seeded into a 3D model, and therefore it is recommended that
35
36 the use of keratinocytes in tissue substitute constructs is limited to passage 3 or less.⁽²⁶⁾
37
38
39
40
41

42 The proper functionality of keratinocytes is important not only for epithelial layer formation,
43
44 but also for epithelial-connective tissue attachment and cell-cell adhesion, which are essential
45
46 for achieving an accurate, functional mucosal substitute. Our data, consistent with data from
47
48 other studies, has confirmed that cells within the 3D models actively synthesised the
49
50 ultrastructural components including desmosomes, hemidesmosomes, and basement
51
52 membrane required for this structural stability.^(27, 28)
53
54
55
56
57
58
59
60

1
2
3 Although collagen I is a non-specific marker of osteogenesis, relatively high levels were
4 expressed in our model compared to other osteogenic genes; this may be due to a number of
5 reasons. Firstly, this marker constitutes the most abundant component of bone extracellular
6 matrix (90% of the organic component) and becomes upregulated during bone formation.⁽²⁹⁾
7
8 Secondly, ascorbic acid was added as a component of the culture medium in order to
9 maintain the osteoblastic phenotype of bone-derived cells; ascorbic acid is known to
10 stimulate of cell growth and collagen synthesis in osteoblasts.⁽³⁰⁾ The hydroxylation of
11 proline residues of procollagen is increased to approximately 40% by ascorbate, which is
12 known to stabilize the collagen triple helix.⁽³¹⁾ Thirdly, although collagen I is the main
13 organic component secreted by osteoblasts, it is also produced in abundance by fibroblasts^{(32,}
14³³⁾, and therefore the fibroblastic component of the model may have contributed to the
15 collagen levels observed.
16
17
18
19
20
21
22
23
24
25
26
27
28

29 We undertook analysis of further osteoblastic markers, including Osteocalcin, Osteopontin,
30 Osteonectin and ALP. ALP, like Collagen I, is expressed in tissues other than bone and
31 therefore its expression cannot be considered specific, although it is synthesised by
32 osteoblasts and has been used to assess osteoblast phenotype and matrix mineralization.⁽³⁴⁾
33
34 Conversely, Osteocalcin, Osteopontin, and Osteonectin are major non-collagenous, bone-
35 specific proteins that play profound roles in bone formation.⁽²⁹⁾ Osteonectin, in particular, is
36 localized to mineralized bone trabeculae and is present at higher concentrations within
37 extracellular matrix than in osteocytes. It selectively binds to collagen I and the resultant
38 osteonectin-collagen complexes initiate mineral phase deposition by binding synthetic apatite
39 crystals and free calcium ions.⁽³⁵⁾ Interestingly, Osteonectin can be demonstrated in active
40 osteoblasts and osteoprogenitor cells as well as in young osteocytes, but not in aged,
41 quiescent osteocytes; the protein is therefore a reliable marker of functional osteoblasts.⁽³⁶⁾
42
43
44
45
46
47
48
49
50
51
52
53
54
55
56
57
58
59
60
61
62
63
64
65
66
67
68
69
70
71
72
73
74
75
76
77
78
79
80
81
82
83
84
85
86
87
88
89
90
91
92
93
94
95
96
97
98
99
100
101
102
103
104
105
106
107
108
109
110
111
112
113
114
115
116
117
118
119
120
121
122
123
124
125
126
127
128
129
130
131
132
133
134
135
136
137
138
139
140
141
142
143
144
145
146
147
148
149
150
151
152
153
154
155
156
157
158
159
160
161
162
163
164
165
166
167
168
169
170
171
172
173
174
175
176
177
178
179
180
181
182
183
184
185
186
187
188
189
190
191
192
193
194
195
196
197
198
199
200
201
202
203
204
205
206
207
208
209
210
211
212
213
214
215
216
217
218
219
220
221
222
223
224
225
226
227
228
229
230
231
232
233
234
235
236
237
238
239
240
241
242
243
244
245
246
247
248
249
250
251
252
253
254
255
256
257
258
259
260
261
262
263
264
265
266
267
268
269
270
271
272
273
274
275
276
277
278
279
280
281
282
283
284
285
286
287
288
289
290
291
292
293
294
295
296
297
298
299
300
301
302
303
304
305
306
307
308
309
310
311
312
313
314
315
316
317
318
319
320
321
322
323
324
325
326
327
328
329
330
331
332
333
334
335
336
337
338
339
340
341
342
343
344
345
346
347
348
349
350
351
352
353
354
355
356
357
358
359
360
361
362
363
364
365
366
367
368
369
370
371
372
373
374
375
376
377
378
379
380
381
382
383
384
385
386
387
388
389
390
391
392
393
394
395
396
397
398
399
400
401
402
403
404
405
406
407
408
409
410
411
412
413
414
415
416
417
418
419
420
421
422
423
424
425
426
427
428
429
430
431
432
433
434
435
436
437
438
439
440
441
442
443
444
445
446
447
448
449
450
451
452
453
454
455
456
457
458
459
460
461
462
463
464
465
466
467
468
469
470
471
472
473
474
475
476
477
478
479
480
481
482
483
484
485
486
487
488
489
490
491
492
493
494
495
496
497
498
499
500
501
502
503
504
505
506
507
508
509
510
511
512
513
514
515
516
517
518
519
520
521
522
523
524
525
526
527
528
529
530
531
532
533
534
535
536
537
538
539
540
541
542
543
544
545
546
547
548
549
550
551
552
553
554
555
556
557
558
559
560
561
562
563
564
565
566
567
568
569
570
571
572
573
574
575
576
577
578
579
580
581
582
583
584
585
586
587
588
589
590
591
592
593
594
595
596
597
598
599
600
601
602
603
604
605
606
607
608
609
610
611
612
613
614
615
616
617
618
619
620
621
622
623
624
625
626
627
628
629
630
631
632
633
634
635
636
637
638
639
640
641
642
643
644
645
646
647
648
649
650
651
652
653
654
655
656
657
658
659
660
661
662
663
664
665
666
667
668
669
670
671
672
673
674
675
676
677
678
679
680
681
682
683
684
685
686
687
688
689
690
691
692
693
694
695
696
697
698
699
700
701
702
703
704
705
706
707
708
709
710
711
712
713
714
715
716
717
718
719
720
721
722
723
724
725
726
727
728
729
730
731
732
733
734
735
736
737
738
739
740
741
742
743
744
745
746
747
748
749
750
751
752
753
754
755
756
757
758
759
760
761
762
763
764
765
766
767
768
769
770
771
772
773
774
775
776
777
778
779
780
781
782
783
784
785
786
787
788
789
790
791
792
793
794
795
796
797
798
799
800
801
802
803
804
805
806
807
808
809
810
811
812
813
814
815
816
817
818
819
820
821
822
823
824
825
826
827
828
829
830
831
832
833
834
835
836
837
838
839
840
841
842
843
844
845
846
847
848
849
850
851
852
853
854
855
856
857
858
859
860
861
862
863
864
865
866
867
868
869
870
871
872
873
874
875
876
877
878
879
880
881
882
883
884
885
886
887
888
889
890
891
892
893
894
895
896
897
898
899
900
901
902
903
904
905
906
907
908
909
910
911
912
913
914
915
916
917
918
919
920
921
922
923
924
925
926
927
928
929
930
931
932
933
934
935
936
937
938
939
940
941
942
943
944
945
946
947
948
949
950
951
952
953
954
955
956
957
958
959
960
961
962
963
964
965
966
967
968
969
970
971
972
973
974
975
976
977
978
979
980
981
982
983
984
985
986
987
988
989
990
991
992
993
994
995
996
997
998
999
1000

1
2
3 suggests that HOBs maintained their phenotypic characteristics in spite of a protracted culture
4
5 period of 2 months.
6

7 The expression of all osteoblast-associated molecules varies over the different stages of
8
9 bone development, and therefore the expression profiles observed in our models, which
10
11 were cultured over a relatively short period compared to that of normal human bone
12
13 turnover may vary somewhat to that observed *in vivo*. For example, ALP increases in the
14
15 initial stages of bone formation, yet decreases as mineralization progresses, whereas
16
17 osteopontin is first detected in young bone, whilst Osteocalcin appears towards the end of
18
19 the mineralization process.⁽³⁷⁾
20
21
22
23
24
25
26

27 **5. Conclusion**

28
29 This study demonstrates that tissue engineered tri-layered reconstructs based on primary
30
31 human alveolar osteoblasts cultured in porous hydroxyapatite/tricalcium phosphate scaffolds
32
33 adhered to collagen-embedded gingival fibroblasts overlain with primary gingival
34
35 keratinocytes cultured at the air/liquid interface, were able to mimic the native alveolar bone
36
37 and overlying full-thickness mucosal structures. The engineered combined hard and soft
38
39 tissue provides scope to act as a valuable alternative to 2D and animal models for various *in*
40
41 *vitro* and potential *in vivo* applications. Further experiments are underway to assess the
42
43 suitability of this 3D model for *in vitro* evaluation of bone invasion of oral cancer as well as
44
45 development of *in vitro* tissue engineered models of osseointegrated dental implants using the
46
47 3D composite bone mucosal system.
48
49
50
51
52
53
54

55 **Acknowledgement**

56
57
58
59
60

1
2
3 The authors would like to thank Abdurahman El-Awa, Yusuf Alzayani, Ei Leen Lim, Claire
4 Field, and all the other surgeons who provided us with bone chips and oral mucosa tissue. We
5 acknowledge Kirsty Franklin for her help and support in the tissue culture laboratory, Chris
6 Hill for his assistance with electron microscopy services, Rebecca Goodchild and Ceramisys
7 LTD, UK for providing the bone scaffolds.
8
9
10
11
12

13 14 15 16 **Conflict of interests**

17
18
19 The authors declare that there is no conflict of interests regarding the publication of this
20 paper.
21
22
23
24
25
26
27
28
29
30
31
32
33
34
35
36
37
38
39
40
41
42
43
44
45
46
47
48
49
50
51
52
53
54
55
56
57
58
59
60

References

1. Lanza, R.P., Langer, R.S., and Vacanti, J. Principles of tissue engineering. Fourth edition. ed: Amsterdam : Academic Press, 2014.
2. Rouwkema, J., Gibbs, S., Lutolf, M.P., Martin, I., Vunjak-Novakovic, G., and Malda, J. In vitro platforms for tissue engineering: implications for basic research and clinical translation. *J Tissue Eng Regen Med* **5**, e164, 2011.
3. Khoruzhenko, A.I. 2D- and 3D- cell culture. *Biopolymers and Cell* **27**, 17, 2011.
4. van der Worp, H.B., Howells, D.W., Sena, E.S., Porritt, M.J., Rewell, S., Collins, V., and Macleod, M.R. Can Animal Models of Disease Reliably Inform Human Studies? *PLoS Medicine* **7**, e1000245, 2010.
5. Pallua, N., and Suschek, C.V. Tissue engineering: from lab to clinic. London,Berlin: Springer; 2010.
6. Sun, J., Hou, X.-K., and Zheng, Y.-X. Restore a 9 mm diameter osteochondral defect with gene enhanced tissue engineering followed mosaicplasty in a goat model. *Acta Orthopaedica et Traumatologica Turcica* **50**, 464, 2016.
7. Ruan, S.Q., Yan, L., Deng, J., Huang, W.L., and Jiang, D.M. Preparation of a biphasic composite scaffold and its application in tissue engineering for femoral osteochondral defects in rabbits. *International Orthopaedics*, 1, 2017.
8. Park, C.H., Rios, H.F., Jin, Q., Sugai, J.V., Padial-Molina, M., Taut, A.D., Flanagan, C.L., Hollister, S.J., and Giannobile, W.V. Tissue engineering bone- ligament complexes using fiber- guiding scaffolds. *Biomaterials* 2011.
9. Almela, T., Brook, I., and Moharamzadeh, K. Development of three-dimensional tissue engineered bone-oral mucosal composite models. *J Mater Sci: Mater Med* 27:65, 2016.
10. Moharamzadeh, K., Brook, I., Noort, R., Scutt, A., Smith, K., and Thornhill, M. Development, optimization and characterization of a full-thickness tissue engineered human

- 1
2
3 oral mucosal model for biological assessment of dental biomaterials. *J Mater Sci: Mater Med*
4
5 **19**, 1793, 2008.
6
7
8 11. Rheinwald, J.G., and Green, H. Serial cultivation of strains of human epidermal
9
10 keratinocytes: the formation of keratinizing colonies from single cells. *Cell* **6**, 331, 1975.
11
12 12. Maillhot, J.M., and Borke, J.L. An isolation and in vitro culturing method for human
13
14 intraoral bone cells derived from dental implant preparation sites. *Clinical Oral Implants*
15
16 *Research* **9**, 43, 1998.
17
18 13. Clausen, C., Hermund, N.U., Donatsky, O., and Nielsen, H. Characterization of human
19
20 bone cells derived from the maxillary alveolar ridge. *Clinical Oral Implants Research* **17**,
21
22 533, 2006.
23
24 14. Dongari-Bagtzoglou, A., and Kashleva, H. Development of a highly reproducible three-
25
26 dimensional organotypic model of the oral mucosa. *Nat Protoc* **1**, 2006.
27
28 15. Kriegebaum, U., Mildenerger, M., Mueller-Richter, U.D.A., Klammert, U., Kuebler,
29
30 A.C., and Reuther, T. Tissue engineering of human oral mucosa on different scaffolds: in
31
32 vitro experiments as a basis for clinical applications. *Oral Surgery, Oral Medicine, Oral*
33
34 *Pathology and Oral Radiology* **114**, S190, 2012.
35
36 16. Morgan, P.R., Shirlaw, P.J., Johnson, N.W., Leigh, I.M., and Lane, E.B. Potential
37
38 applications of anti- keratin antibodies in oral diagnosis. *Journal of oral pathology* **16**, 212,
39
40 1987.
41
42 17. Nanci, A. Ten Cate oral histology : development, structure, and function. 8th ed. /
43
44 Antonio Nanci. ed. St. Louis, Mo.: St. Louis, Mo. : Elsevier, 2013.
45
46 18. Tayebi, L., and Moharamzadeh, K. Biomaterials for oral and dental tissue engineering:
47
48 Oxford : Woodhead Publishing, 2017.
49
50
51
52
53
54
55
56
57
58
59
60

- 1
2
3 19. Peppas, N.A., Hilt, J.Z., Khademhosseini, A., and Langer, R. Hydrogels in Biology and
4
5 Medicine: From Molecular Principles to Bionanotechnology. *Advanced Materials* **18**, 1345,
6
7 2006.
8
9
10 20. Rouwkema, J., Rivron, N.C., and van Blitterswijk, C.A. Vascularization in tissue
11
12 engineering. *Trends Biotechnol* **26**, 434, 2008.
13
14 21. Chai, W.L., Moharamzadeh, K., Van Noort, R., Brook, I.M., Emanuelsson, L., and
15
16 Palmquist, A. Development of a novel model for the investigation of implant- soft tissue
17
18 interface. *Journal of Periodontology* **81**, 1187, 2010.
19
20
21 22. Okazaki, M., Yoshimura, K., Suzuki, Y., and Harii, K. Effects of subepithelial fibroblasts
22
23 on epithelial differentiation in human skin and oral mucosa: heterotypically recombined
24
25 organotypic culture model. *Plastic and reconstructive surgery* **112**, 784, 2003.
26
27
28 23. Rakhorst, H., Tra, W., Van Neck, J.W., Van Osch, G., Hovius, S., El Ghalbzouri, A., and
29
30 Hofer, S.O.P. Fibroblasts Accelerate Culturing of Mucosal Substitutes. *Tissue Engineering*
31
32 **12**, 2321, 2006.
33
34
35 24. Wang, Z., Wang, Y., Farhangfar, F., Zimmer, M., and Zhang, Y. Enhanced Keratinocyte
36
37 Proliferation and Migration in Co- culture with Fibroblasts (Keratinocyte Proliferation and
38
39 Migration). *PLoS ONE* **7**, e40951, 2012.
40
41
42 25. El Ghalbzouri, A., Gibbs, S., Lamme, E., Van Blitterswijk, C.A., and Ponec, M. Effect
43
44 of fibroblasts on epidermal regeneration. *British Journal of Dermatology* **147**, 230, 2002.
45
46
47 26. Ng, M.H., Aminuddin, B.S., Hamizah, S., Lynette, C., Mazlyzam, A.L., and Ruszymah,
48
49 B.H.I. Correlation of donor age and telomerase activity with in vitro cell growth and
50
51 replicative potential for dermal fibroblasts and keratinocytes. *Journal of Tissue Viability* **18**,
52
53 109, 2009.
54
55
56
57
58
59
60

- 1
2
3 27. Tra, W.M.W., Van Neck, J.W., Hovius, S.E.R., Perez-Amodio, S., and Van Osch,
4 G.J.V.M. Characterization of a three- dimensional mucosal equivalent: Similarities and
5 differences with native oral mucosa. *Cells Tissues Organs* **195**, 185, 2012.
6
7
8
9
10 28. Chai, W.L., Van Noort, R., Moharamzadeh, K., Brook, I.M., Emanuelsson, L., and
11 Palmquist, A. Ultrastructural analysis of implant- soft tissue interface on a three dimensional
12 tissue- engineered oral mucosal model. *Journal of Biomedical Materials Research - Part A*
13 **100**, 269, 2012.
14
15
16
17
18 29. Allori, A., Sailon, A., and Warren, S. Biological Basis of Bone Formation, Remodeling,
19 and Repair-- Part I: Biochemical Signaling Molecules. *Tissue Engineering*, **14**, 259, 2008.
20
21
22
23 30. Choi, K.-M., Seo, Y.-K., Yoon, H.-H., Song, K.-Y., Kwon, S.-Y., Lee, H.-S., and Park,
24 J.-K. Effect of ascorbic acid on bone marrow- derived mesenchymal stem cell proliferation
25 and differentiation. *Journal of Bioscience and Bioengineering* **105**, 586, 2008.
26
27
28
29 31. Berg, R.A., and Prockop, D.J. The thermal transition of a non- hydroxylated form of
30 collagen. Evidence for a role for hydroxyproline in stabilizing the triple- helix of collagen.
31 *Biochemical and Biophysical Research Communications* **52**, 115, 1973.
32
33
34
35 32. Kishimoto, Y., Saito, N., Kurita, K., Shimokado, K., Maruyama, N., and Ishigami, A.
36 Ascorbic acid enhances the expression of type 1 and type 4 collagen and SVCT2 in cultured
37 human skin fibroblasts. *Biochemical and Biophysical Research Communications* **430**, 579,
38 2013.
39
40
41
42
43
44 33. Schwarz, R.I. Collagen I and the fibroblast: High protein expression requires a new
45 paradigm of post- transcriptional, feedback regulation. *Biochemistry and Biophysics Reports*
46 **3**, 38, 2015.
47
48
49
50
51 34. Masrour Roudsari, J., and Mahjoub, S. Quantification and comparison of bone- specific
52 alkaline phosphatase with two methods in normal and paget's specimens. *Caspian journal of*
53 *internal medicine* **3**, 478, 2012.
54
55
56
57
58
59
60

- 1
2
3 35. Termine, J.D., Kleinman, H.K., Whitson, S.W., Conn, K.M., McGarvey, M.L., and
4
5 Martin, G.R. Osteonectin, a bone- specific protein linking mineral to collagen. *Cell* **26**, 99,
6
7 1981.
8
9
10 36. Jundt, G., Berghäuser, K., Termine, J., and Schulz, A. Osteonectin — a differentiation
11
12 marker of bone cells. *Cell and Tissue Research* **248**, 409, 1987.
13
14 37. Kim, M.-C., Hong, M.-H., Lee, B.-H., Choi, H.-J., Ko, Y.-M., and Lee, Y.-K. Bone
15
16 Tissue Engineering by Using Calcium Phosphate Glass Scaffolds and the Avidin– Biotin
17
18 Binding System. *The Journal of the Biomedical Engineering Society* **43**, 3004, 2015.
19
20
21
22
23
24
25
26
27
28
29
30
31
32
33
34
35
36
37
38
39
40
41
42
43
44
45
46
47
48
49
50
51
52
53
54
55
56
57
58
59
60

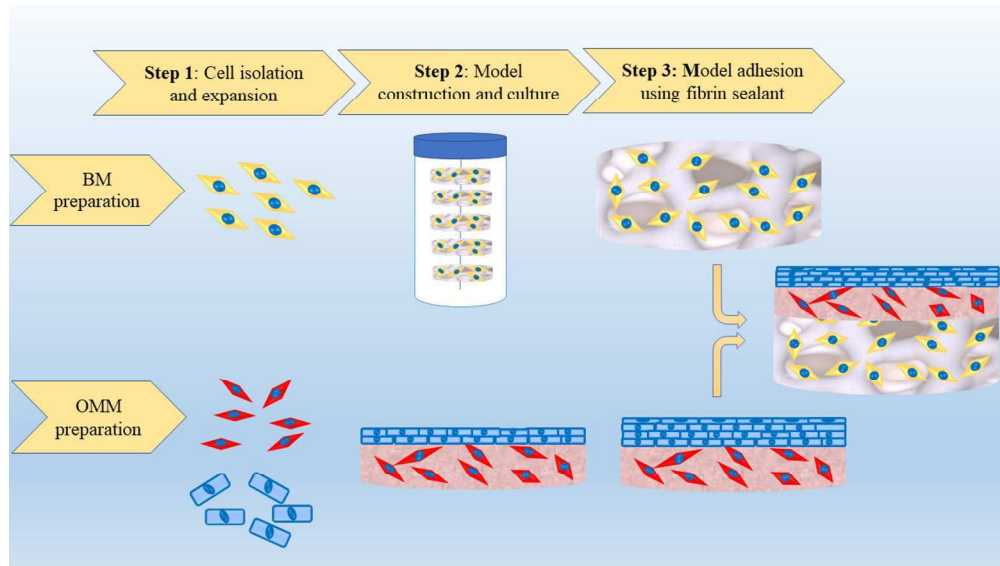


Figure 1. Schematic illustration of the preparation of OMM, BM, and ABMM. The procedure involved 3 main steps. First; HAOBs, NHOFs, and NHOKs were isolated from oral tissues and cultivated in monolayer culture. Second; BMs were prepared by seeding HAOBs in HA/TCP scaffold and cultured in spinner bioreactor while OMMs were prepared from fibroblast-populated collagen gel and air liquid interface culture oral keratinocytes. Third; Combination of BM and OMM using adhesive fibrin to form ABMM.

338x190mm (300 x 300 DPI)

1
2
3
4
5
6
7
8
9
10
11
12
13
14
15
16
17
18
19
20
21
22
23
24
25
26
27
28
29
30
31
32
33
34
35
36
37
38
39
40
41
42
43
44
45
46
47
48
49
50
51
52
53
54
55
56
57
58
59
60

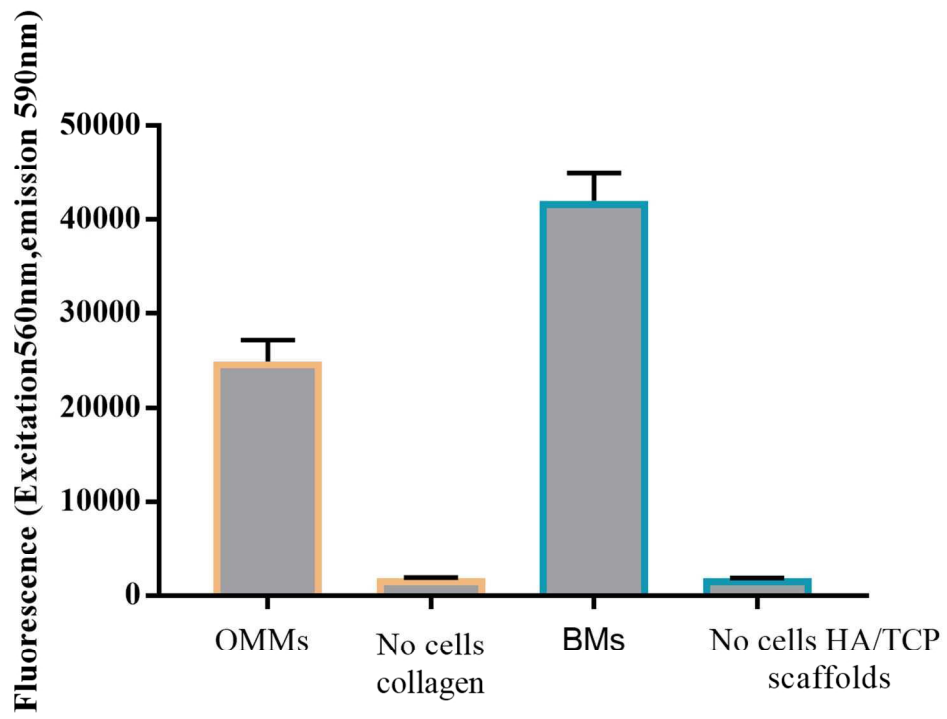


Figure 2. Vitality assessment of OMMs and BMs. The figure shows the activity of HAOBs within HA/TCP scaffold as well as NHOFs and NHOKs in OMMs after 17 days of culture.

107x83mm (300 x 300 DPI)

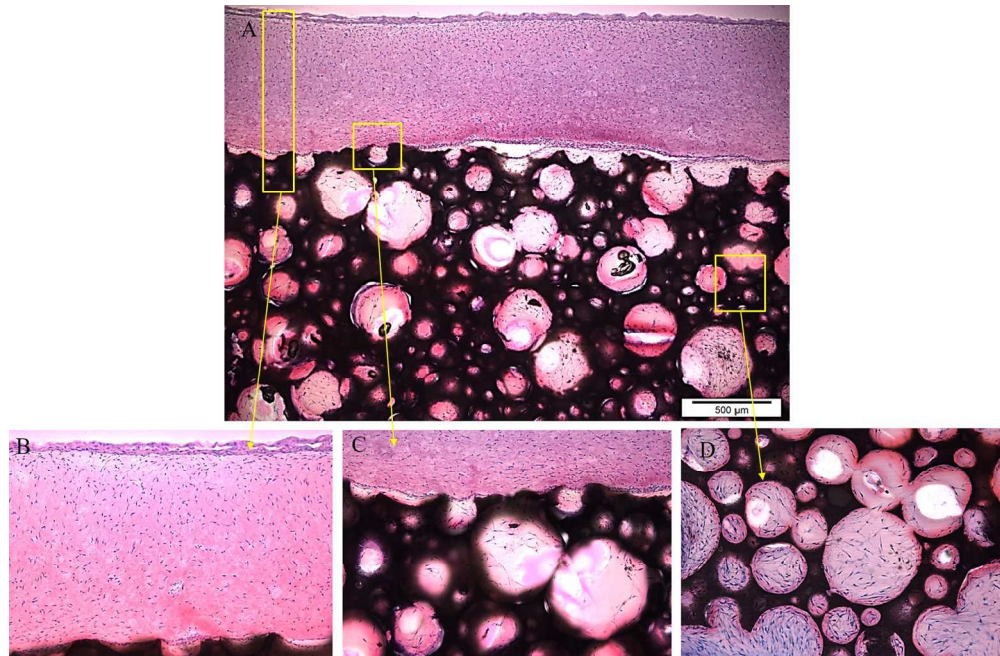


Figure 3. H&E-stained histological sections of ABMM showing (A) full-thickness multi-layered bone and mucosa; and magnified images of (B) oral mucosa part; (C) bone-mucosal interface; and (D) bony part showing the pores of the scaffold filled with osteoblasts and extracellular matrix (Original magnification A \times 4; B, C, and D \times 10).

143x93mm (300 x 300 DPI)

1
2
3
4
5
6
7
8
9
10
11
12
13
14
15
16
17
18
19
20
21
22
23
24
25
26
27
28
29
30
31
32
33
34
35
36
37
38
39
40
41
42
43
44
45
46
47
48
49
50
51
52
53
54
55
56
57
58
59
60

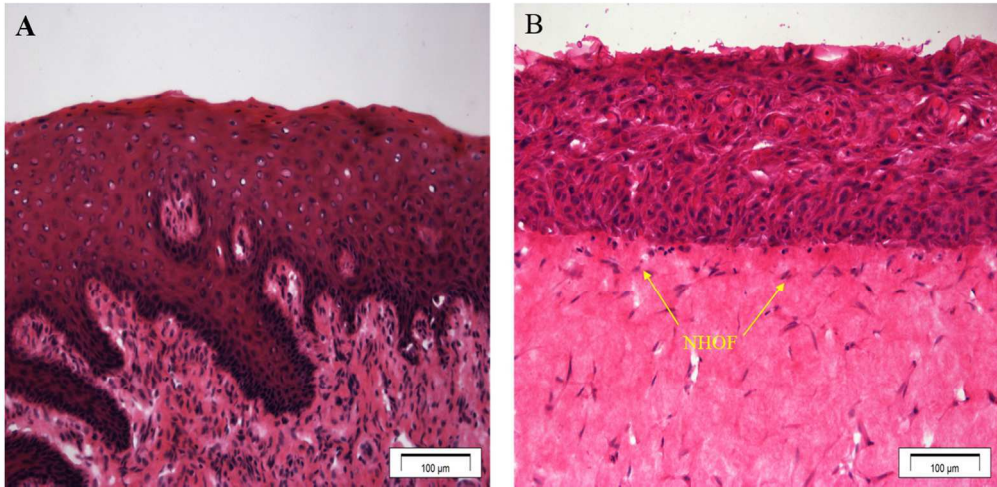


Figure 4. H&E-stained histological sections of (A) NOM; and (B) OMM showing a well-differentiated stratified squamous epithelial layer with viable fibroblasts scattered in the connective tissue layer (Original magnification $\times 20$).

123x60mm (300 x 300 DPI)

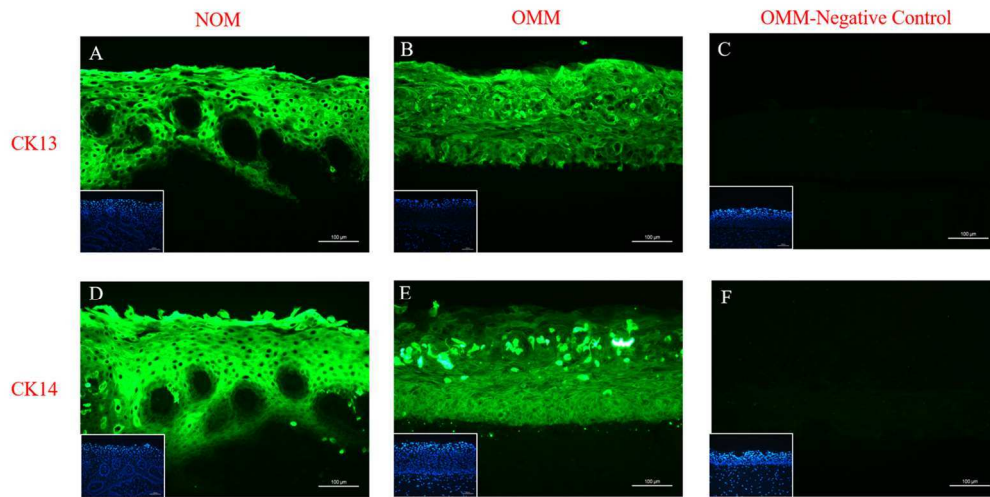


Figure 5. Immunofluorescent staining of the oral mucosa showing (A and D) both epithelial markers CK13 and CK14 were well detected in the NOM; (B and E) strong expression of CK13 and CK14 in the OMM; and (C, F) negative control (Original magnification $\times 20$; the lower left boxes are DAPI stain).

127x63mm (300 x 300 DPI)

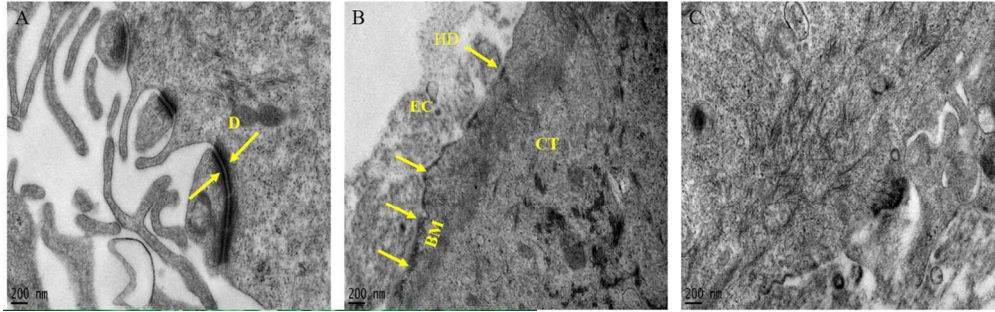


Figure 6. Ultrastructural analysis of the OMM by transmission electron microscopy showing (A) numerous desmosomes (D) between adjacent epithelial cells; (B) basement membrane (BM) formed all along the interface between the epithelial cell (EC) and connective tissue (CT) with the presence of hemidesmosomes (HD); and (C) newly synthesized collagen I fibrils in the connective tissue (Original magnification $\times 50000$).

127x39mm (300 x 300 DPI)

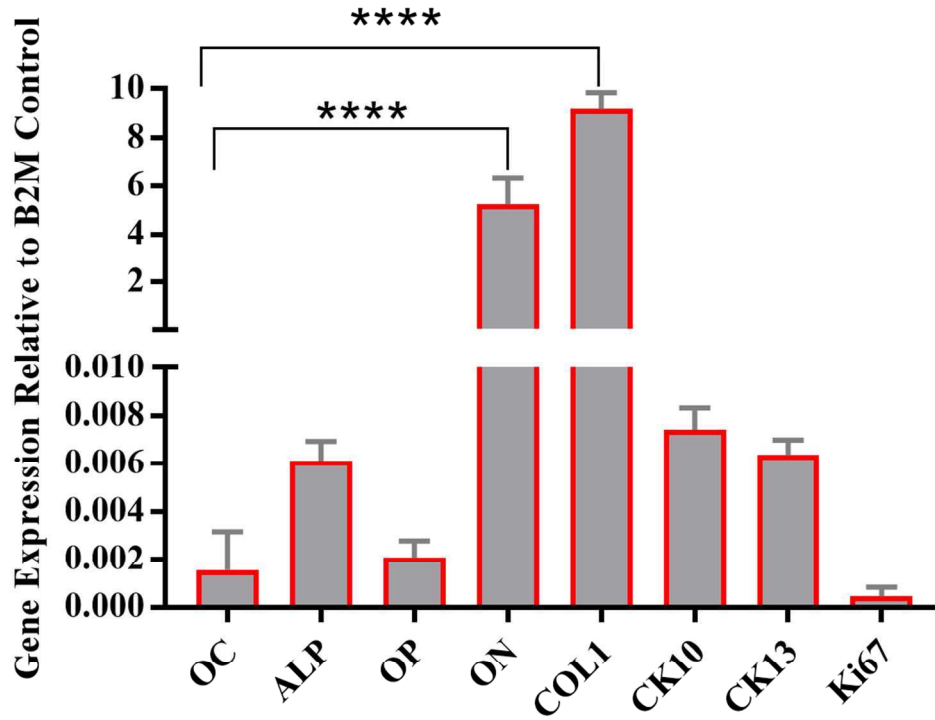


Figure 7. The gene expression of HAOBs and NHOKs in the ABMM as evaluated with PCR analysis. The osteogenic markers; OC, ALP, OP, ON, and COL1, in addition to the epithelial markers; CK10, CK13 were detected. Statistical significance was determined as $p < 0.05$ from control (**** $P < 0.0001$).

97x78mm (300 x 300 DPI)

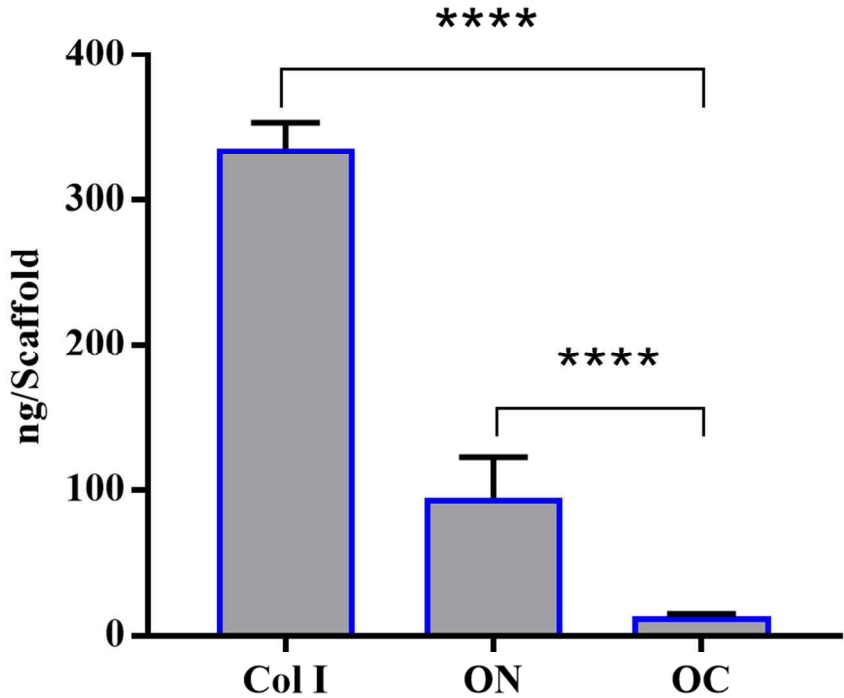


Figure 8. Protein expression of Collagen I, Osteonectin, and Osteocalcin in ABMM analyzed by ELISA. Statistical significance was determined as $p < 0.05$ (**** $P < 0.0001$).

87x69mm (300 x 300 DPI)

1
2
3 **Figure legends:**

4 **Figure 1. Schematic illustration of the preparation of OMM, BM, and ABMM.** The
5 procedure involved 3 main steps. First; HAOBs, NHOFs, and NHOKs were isolated from
6 oral tissues and cultivated in monolayer culture. Second; BMs were prepared by seeding
7 HAOBs in HA/TCP scaffold and cultured in spinner bioreactor while OMMs were prepared
8 from fibroblast-populated collagen gel and air liquid interface culture oral keratinocytes.
9
10
11
12
13
14
15
16
17
18
19
20
21
22
23
24
25
26
27
28
29
30
31
32
33
34
35
36
37
38
39
40
41
42
43
44
45
46
47
48
49
50
51
52
53
54
55
56
57
58
59
60
Third; Combination of BM and OMM using adhesive fibrin to form ABMM.

Figure 2. Vitality assessment of OMMs and BMs. The figure shows the activity of HAOBs
within HA/TCP scaffold as well as NHOFs and NHOKs in OMMs after 17 days of culture.

Figure 3. H&E-stained histological sections of ABMM showing (A) full-thickness multi-
layered bone and mucosa; and magnified images of (B) oral mucosa part; (C) bone-mucosal
interface; and (D) bony part showing the pores of the scaffold filled with osteoblasts and
extracellular matrix (Original magnification A \times 4; B, C, and D \times 10).

Figure 4. H&E-stained histological sections of (A) NOM; and (B) OMM showing a well-
differentiated stratified squamous epithelial layer with viable fibroblasts scattered in the
connective tissue layer (Original magnification \times 20).

Figure 5. Immunofluorescent staining of the oral mucosa showing (A and D) both
epithelial markers CK13 and CK14 were well detected in the NOM; (B and E) strong
expression of CK13 and CK14 in the OMM; and (C, F) negative control (Original
magnification \times 20; the lower left boxes are DAPI stain).

Figure 6. Ultrastructural analysis of the OMM by transmission electron microscopy
showing (A) numerous desmosomes (D) between adjacent epithelial cells; (B) basement
membrane (BM) formed all along the interface between the epithelial cell (EC) and

1
2
3 connective tissue (CT) with the presence of hemidesmosomes (HD); and (C) newly
4
5 synthesized collagen I fibrils in the connective tissue (Original magnification $\times 50000$).
6
7

8 **Figure 7. The gene expression of HAOBs and NHOKs in the ABMM as evaluated**
9 **with PCR analysis.** The osteogenic markers; OC, ALP, OP, ON, and COL1, in addition to
10 the epithelial markers; CK10, CK13 were detected. Statistical significance was determined
11 as $p < 0.05$ from control (**** $P < 0.0001$).
12
13
14
15

16
17 **Figure 8.** Protein expression of Collagen I, Osteonectin, and Osteocalcin in ABMM analyzed
18 by ELISA. Statistical significance was determined as $p < 0.05$ (**** $P < 0.0001$).
19
20
21
22
23
24
25
26
27
28
29
30
31
32
33
34
35
36
37
38
39
40
41
42
43
44
45
46
47
48
49
50
51
52
53
54
55
56
57
58
59
60